ATP-dependent Adenophostin Activation of Inositol 1,4,5-Trisphosphate Receptor Channel Gating

Kinetic Implications for the Durations of Calcium Puffs in Cells

Don-On Daniel Mak, Sean McBride, and J. Kevin Foskett

From the Department of Physiology, University of Pennsylvania, Philadelphia, Pennsylvania 19104

ABSTRACT The inositol 1,4,5-trisphosphate ($InsP_3$) receptor ($InsP_3R$) is a ligand-gated intracellular Ca^{2+} release channel that plays a central role in modulating cytoplasmic free Ca^{2+} concentration ($[Ca^{2+}]_i$). The fungal metabolite adenophostin A (AdA) is a potent agonist of the $InsP_3R$ that is structurally different from $InsP_3$ and elicits distinct calcium signals in cells. We have investigated the effects of AdA and its analogues on single-channel activities of the $InsP_3R$ in the outer membrane of isolated *Xenopus laevis* oocyte nuclei. $InsP_3R$ activated by either AdA or $InsP_3$ have identical channel conductance properties. Furthermore, AdA, like $InsP_3$, activates the channel by tuning Ca^{2+} inhibition of gating. However, gating of the AdA-liganded $InsP_3R$ has a critical dependence on cytoplasmic ATP free acid concentration not observed for $InsP_3$-liganded channels. Channel gating activated by AdA is indistinguishable from that elicited by $InsP_3$ in the presence of 0.5 mM ATP, although the functional affinity of the channel is 60-fold higher for AdA. However, in the absence of ATP, gating kinetics of AdA-liganded $InsP_3R$ were very different. Channel open time was reduced by 50%, resulting in substantially lower maximum open probability than channels activated by AdA in the presence of ATP, or by $InsP_3$ in the presence or absence of ATP. Also, the higher functional affinity of $InsP_3R$ for AdA than for $InsP_3$ is nearly abolished in the absence of ATP. Low affinity AdA analogues furanophostin and ribophostin activated $InsP_3R$ channels with gating properties similar to those of AdA. These results provide novel insights for interpretations of observed effects of AdA on calcium signaling, including the mechanisms that determine the durations of elementary Ca^{2+} release events in cells. Comparisons of single-channel gating kinetics of the $InsP_3R$ activated by $InsP_3$, AdA, and its analogues also identify molecular elements in $InsP_3R$ ligands that contribute to binding and activation of channel gating.

KEY WORDS: patch-clamp • *Xenopus* oocyte • single-channel electrophysiology • intracellular calcium signaling • calcium release channel

INTRODUCTION

The inositol 1,4,5-trisphosphate receptor ($InsP_3R$)[1] is an intracellular Ca^{2+} release channel that is localized to the endoplasmic reticulum. It plays a central role in the modulation of free cytoplasmic Ca^{2+} concentration ($[Ca^{2+}]_i$) by a ubiquitous cellular signaling system involving activation of phospholipase C. Binding of extracellular ligands to plasma membrane receptors generates $InsP_3$, which diffuses through the cytoplasm to bind and activate the $InsP_3R$, releasing Ca^{2+} from the endoplasmic reticulum lumen into the cytoplasm to raise $[Ca^{2+}]_i$. Complex $InsP_3$-mediated calcium signals in the form of repetitive spikes, oscillations, and propagating waves initiated from specific locations in the cell have been observed in many cell types (Bootman and Berridge, 1995; Toescu, 1995). The molecular bases of these spatially and temporally complex calcium signals include cytoplasmic and organellar Ca^{2+} buffering systems, location of intracellular Ca^{2+} stores and, most importantly, the properties of the $InsP_3R$. The $InsP_3R$ Ca^{2+} release channel is highly regulated by complex mechanisms that are still only poorly understood, including cooperative activation by $InsP_3$ (Meyer et al., 1988; Finch et al., 1991; Mak et al., 1998) and biphasic concentration-dependent feedback from the permeant Ca^{2+} ion (Iino, 1990; Bezprozvanny et al., 1991; Finch et al., 1991; Mak et al., 1998). Three isoforms of $InsP_3R$ (types 1, 2, and 3) as products of different genes with alternatively spliced isoforms have been identified and sequenced (Mignery et al., 1989; Mikoshiba, 1993). The $InsP_3R$ isoforms all have ~2,700 amino acid residues contained in three ($InsP_3$-binding, regulatory [modulatory], and transmembrane channel-forming) domains (Mignery et al., 1989; Mikoshiba, 1993). The sequences of the regulatory domains of all $InsP_3R$ isoforms include putative ATP-binding site(s) (Mikoshiba, 1993). ATP has been shown to bind to the $InsP_3R$

Address correspondence to Dr. J. Kevin Foskett, Department of Physiology, B400 Richards Building, University of Pennsylvania, Philadelphia, PA 19104-6085. Fax: (215) 573-6808;
E-mail: foskett@mail.med.upenn.edu

[1]*Abbreviations used in this paper:* AdA, adenophostin A; $[Ca^{2+}]_i$, cytoplasmic free Ca^{2+} concentration; Fur, furanophostin; $InsP_3$, inositol 1,4,5-trisphosphate; $InsP_3R$, $InsP_3$ receptor; pdf, probability density function; Rib, ribophostin.

(Maeda et al., 1991) and regulate $InsP_3R$-mediated Ca^{2+} release in permeabilized cells (Ferris et al., 1990; Iino, 1991; Bezprozvanny and Ehrlich, 1993; Missiaen et al., 1997; Landolfi et al., 1998; Mak et al., 1999; Meas et al., 2000). At the single-channel level, ATP activates $InsP_3$-dependent $InsP_3R$ gating (Bezprozvanny and Ehrlich, 1993; Mak et al., 1999; Hagar and Ehrlich, 2000). Activation of the *Xenopus* type 1 $InsP_3R$ channel by ATP is accomplished by allosteric tuning of the affinity of the Ca^{2+} activation sites, enabling $InsP_3$-dependent channel gating to be more sensitive to activation by cytoplasmic Ca^{2+} (Mak et al., 1999).

Adenophostin A (AdA), a fungal glyconucleotide metabolite (Takahashi et al., 1994), and its analogues (Marchant et al., 1997; Shuto et al., 1998; Beecroft et al., 1999) were recently discovered as potent agonists of the $InsP_3R$. Although their molecular structures are significantly different from those of $InsP_3$ and its analogues (Irvine et al., 1984; Fig. 1), they activate the channel by interactions with the $InsP_3$ binding site (Glouchankova et al., 2000). AdA is 10–80-fold more potent than $InsP_3$ in binding to the $InsP_3R$ and stimulating $InsP_3R$-mediated Ca^{2+} release, and it is metabolically stable (Takahashi et al., 1994; Hirota et al., 1995; Murphy et al., 1997). AdA has been applied in studies of the $InsP_3R$ and its regulation (Missiaen et al., 1998; He et al., 1999; Adkins et al., 2000; Jellerette et al., 2000; Kashiwayanagi et al, 2000; Vanlingen et al., 2000), Ca^{2+} release mediated by $InsP_3R$ (Marchant and Parker, 1998; Bird et al., 1999), and Ca^{2+} entry due to depletion of intracellular Ca^{2+} stores (DeLisle et al., 1997; Hartzell et al., 1997; Huang et al., 1998; Broad et al., 1999; Gregory et al., 1999; Machaca and Hartzell, 1999). Compared with $InsP_3$, AdA induced temporally and spatially different calcium signals (Marchant and Parker, 1998; Bird et al., 1999) and Ca^{2+}-dependent Cl^- currents (Hartzell et al., 1997; Machaca and Hartzell, 1999) in *Xenopus* oocytes. Furthermore, AdA, but not $InsP_3$, activated Ca^{2+} entry with an apparent lack of Ca^{2+} release from stores (DeLisle et al., 1997). These observations suggested that the effects of AdA on calcium signaling were different from those expected if it was simply a more potent equivalent of $InsP_3$. However, there have been no direct examinations of the single-channel properties of $InsP_3R$ activated by AdA.

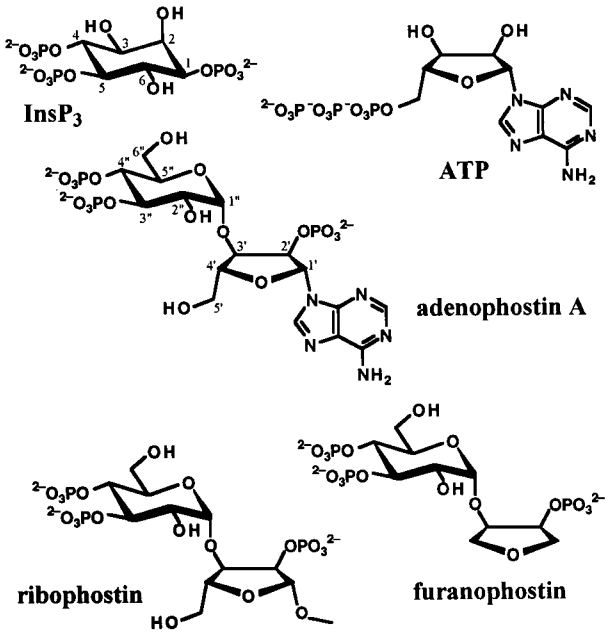

FIGURE 1. Molecular structures of various $InsP_3R$-binding ligands.

Whereas AdA has a significantly higher affinity for binding to the $InsP_3R$ and a higher potency to activate the channel than $InsP_3$, ribophostin (Rib) and furanophostin (Fur) (Marchant et al., 1997; Shuto et al., 1998), structural analogues of AdA (Fig. 1), have binding affinities and activating potencies that are comparable to that of $InsP_3$. The relationships between the distinct binding affinities of these various ligands and the detailed gating properties of the $InsP_3R$ channel they elicit are unknown. The molecular structural feature that is unique to AdA and not shared by its less potent analogues is the adenine moiety linked to the ribose ring, which has structural resemblance to that of ATP (Fig. 1). Nevertheless, it has been reported that AdA does not bind to glutathione-S-transferase fusion polypeptides containing the putative ATP binding sequences of the type 1 $InsP_3R$ (Maes et al., 1999). Thus, the molecular determinants involved in the high affinity interaction of AdA with the $InsP_3R$ are still unclear.

The unique cytoplasmic calcium signals elicited by activation of the $InsP_3R$ with different ligands suggest that a detailed understanding of the mechanisms of action of AdA and its analogues could provide important novel insights into the molecular basis for the linkage between ligand binding and activation of the $InsP_3R$ channel. Here, we have performed a systematic investigation of the effects of AdA and its analogues on the single-channel activities of the $InsP_3R$. We have previously applied the patch-clamp technique to the outer membrane of isolated *Xenopus laevis* oocyte nuclei to study extensively the single-channel properties of the endogenous type 1 $InsP_3R$ in its native membrane environment under rigorously controlled experimental conditions (Mak and Foskett, 1994, 1997, 1998; Mak et al., 1998, 1999). Here we characterize the conduction and channel gating properties of single $InsP_3R$ channels activated by AdA and its analogues, Rib and Fur, in the presence of a wide range of cytoplasmic Ca^{2+}, ligand, and ATP concentrations. Our studies demonstrate that the channel conductance properties are identical for $InsP_3R$ channels activated by either AdA or $InsP_3$. However, gating of the $InsP_3R$ activated by AdA or its analogues has a

critical dependence on cytoplasmic ATP free acid concentration that is not observed for $InsP_3$-liganded channels. Channel gating activated by AdA is indistinguishable from that elicited by $InsP_3$ in the presence of 0.5 mM cytoplasmic free ATP, although the functional affinity of the channel is ~60-fold higher for AdA. However, the AdA-liganded channel exhibits very different channel gating kinetics in the absence of cytoplasmic free ATP. The channel open time is reduced by nearly 50% when the channel is activated by AdA in the absence of ATP, resulting in a substantially lower maximum open probability than channels activated by AdA in the presence of ATP, or by $InsP_3$ in the presence or absence of ATP. Furthermore, the higher functional affinity of AdA compared with $InsP_3$ is nearly abolished in the absence of ATP. The low affinity AdA analogues Fur and Rib activated channels with gating properties similar to those of AdA in either the presence or absence of ATP. Our study reveals a prominent role of ATP as an allosteric regulator of the $InsP_3R$ channel, and it provides novel insights for interpretations of observed effects of AdA on intracellular calcium signaling. In particular, the effects of AdA on the kinetics of channel gating suggest novel mechanisms that determine the durations of elementary Ca^{2+} release events in cells. Comparisons of the single-channel gating kinetics of the $InsP_3R$ activated by $InsP_3$, AdA, and its analogues have also enabled identification of molecular structural elements in $InsP_3R$ ligands that contribute to their ability to bind and activate channel gating.

MATERIALS AND METHODS

Patch-clamping the Oocyte Nucleus

Patch-clamp experiments were performed using isolated *Xenopus* oocyte nuclei as described previously (Mak and Foskett, 1994, 1997, 1998; Mak et al., 1998). In brief, stage V or VI oocytes, which express only a single $InsP_3R$ isoform (type 1) and lacks other (e.g., ryanodine receptor) Ca^{2+} release channels (Kume et al., 1993), were opened mechanically just before use. The nucleus was separated from the cytoplasm and transferred to a dish on the stage of a microscope for patch-clamping. Experiments were performed in the "on-nucleus" configuration, with the solution in the perinuclear lumen between the outer and inner nuclear membranes in apparent equilibrium with the bath solution (Mak and Foskett, 1994), and the cytoplasmic aspect of the $InsP_3R$ channel facing into the patch pipet. Experiments were performed at room temperature with the pipet electrode at +20 mV relative to the reference bath electrode.

Data Acquisition and Analysis

Single-channel currents were amplified by an Axopatch-1D amplifier (Axon Instruments, Inc.) with antialiasing filtering at 1 kHz, digitized at 5 kHz, and recorded by Pulse+PulseFit software (HEKA Elektronik). The patch-clamped *Xenopus* $InsP_3R$ inactivates with a time constant of ~30 s after its activation by $InsP_3$ (Mak and Foskett, 1997). Similar inactivation was observed in this study when the channels were activated by AdA. As inactivation was generally abrupt with no detectable change in channel kinetics up to the disappearance of channel activity (Mak and Foskett, 1997), current traces obtained during the entire period the channels were active were analyzed (Mak and Foskett, 1998; Mak et al., 1998). Channel opening and closing events were identified with a 50% threshold, and channel open probability P_o and dwell time distribution evaluated using TAC software (Bruxton). Current traces exhibiting one $InsP_3R$ channel, or two $InsP_3R$ channels determined to be identical and independently gated (Mak and Foskett, 1997), were used for P_o evaluation, whereas only current traces with a single $InsP_3R$ channel were used for dwell time analyses. Each set of open and closed dwell time histograms was derived from one patch-clamp current record of a single active $InsP_3R$ channel. The probability density function (pdf) was fitted to the histograms by the maximum likelihood method (Sigworth and Sine, 1987).

The number of channels in the membrane patch was assumed to be the maximum number of open channel current levels observed throughout the current record. Assuming there are n identical and independent channels in the membrane patch, and each channel is Markovian with open probability of P_o and open duration distribution characterized by a single exponential component of time constant τ^o, the mean dwell time of highest channel current level is τ^o/n. If T is the minimum duration of an open event that is detectable in the experimental system, i.e., only events with duration $>T$ will have amplitudes greater than the 50% threshold after filtering, then the rate of detection of the highest current level:

$$R_n = \frac{n(P_o)^n}{\tau^o}\left[\exp-\left(\frac{nT}{\tau^o}\right)\right]. \quad (1)$$

In our patch-clamp set up, T was empirically determined to be ~0.2 ms using test pulses of variable duration. τ^o of $InsP_3R$ channels is ~3–15 ms over the range of experimental conditions used (Mak et al., 1998). In experimental conditions with $P_o > 0.1$, only current records with longer than 10 s of $InsP_3R$ channel activities were used. Because 10 s $\gg 1/R_3$, there is little uncertainty in the number of channels in the current traces used. In experimental conditions with $P_o < 0.1$, only current records exhibiting one open channel current level with record duration $> 5/R_2$ were used, to ensure that they were truly single-channel records.

Each data point shown is the mean of results from at least four separate patch-clamp experiments performed under the same conditions. Error bars indicate the SEM. Theoretical Hill equation curves were fitted to experimental P_o data using IgorPro (WaveMetrics).

Solutions for Patch-clamp Experiments

All patch-clamp experiments were performed with solutions containing 140 mM KCl and 10 mM HEPES, with pH adjusted to 7.1 using KOH. By using K^+ as the current carrier and appropriate quantities of the high affinity Ca^{2+} chelator, BAPTA (1,2-bis[*O*-aminophenoxy] ethane-*N,N,N′,N′*-tetraacetic acid; 100–1,000 μM; from Molecular Probes), or the low affinity Ca^{2+} chelator, 5,5′-dibromo BAPTA (100–400 μM; Molecular Probes), or ATP (0.5 mM) alone to buffer Ca^{2+} in the experimental solutions, free Ca^{2+} concentrations in our experimental solutions were tightly controlled. Total Ca^{2+} content (5–330 μM) in the solutions was determined by induction-coupled plasma mass spectrometry (Mayo Medical Laboratory). Free $[Ca^{2+}]$ was calculated using the Maxchelator software (C. Patton, Stanford University, Stanford, CA). The free $[Ca^{2+}]$ of the solutions was verified by measurements using Ca^{2+}-selective minielectrodes (Baudet et al., 1994) and found to agree with the calculated $[Ca^{2+}]$ to within the accuracy of the electrode measurement (10%). The bath solutions used in all experiments had 140 mM KCl, 10 mM Hepes,

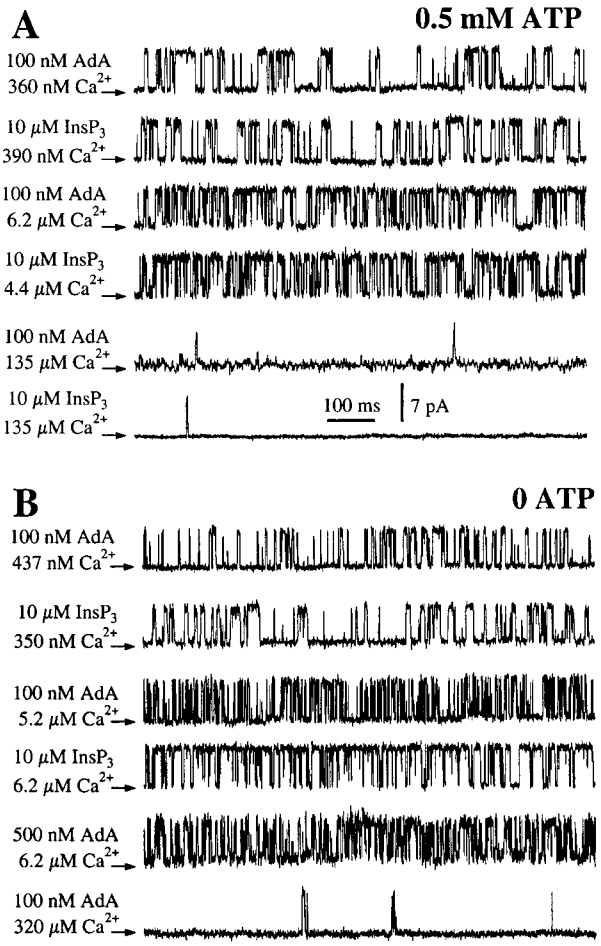

FIGURE 2. Typical single-channel current traces of *X*-InsP$_3$R-1 in various $[Ca^{2+}]_i$, activated by InsP$_3$ or AdA as indicated. Arrows indicate the closed channel current levels. (A) In the presence of 0.5 mM ATP. (B) In the absence of ATP.

380 μM $CaCl_2$, 500 μM BAPTA ($[Ca^{2+}]$ = 500 nM), and pH 7.1. Pipet solutions, to which the cytoplasmic aspects of the channels were exposed, contained either 0 or 0.5 mM of Na_2ATP (Sigma-Aldrich), various concentration of InsP$_3$ (Molecular Probes), AdA, Rib, or Fur (Calbiochem), as stated. All reagents were used without further purification. Because Mg^{2+} was absent from the experimental solutions, ATP mostly existed in free acid forms (ATP^{4-}, ATP^{3-}). We previously demonstrated that ATP free acid, not MgATP complex, was responsible for ATP regulation of InsP$_3$R gating (Mak et al., 1999).

RESULTS

Properties of AdA-liganded InsP$_3$R Channels in the Presence of 0.5 mM Cytoplasmic Free ATP

To compare the single-channel conductance and gating properties of the *Xenopus* type 1 InsP$_3$R (*X*-InsP$_3$R-1) activated by AdA with those activated by InsP$_3$, we performed patch-clamp experiments on the outer membrane of nuclei isolated from *Xenopus* oocytes using the same experimental conditions employed in our previous studies (Mak and Foskett, 1994, 1997; Mak et al., 1998), but with AdA instead of InsP$_3$ as the agonist. With cytoplasmic ATP free acid concentration ([ATP]) of 0.5 mM, the conductance properties and gating kinetics of the *X*-InsP$_3$R-1 channel activated by saturating concentrations of either AdA (100 nM) or InsP$_3$ (10 μM) were indistinguishable in all cytoplasmic free Ca^{2+} concentrations ($[Ca^{2+}]_i$) examined (Fig. 2 A). In addition, all AdA-liganded *X*-InsP$_3$R-1 channels observed in our experiments inactivated despite the continuous presence of AdA in the pipet solution, with durations of channel activity that were comparable to those observed for InsP$_3$-liganded channels (Mak and Foskett, 1997).

The open probability (P_o) of the InsP$_3$-liganded channel varies with $[Ca^{2+}]_i$ in a biphasic manner (Mak et al., 1998). To determine the $[Ca^{2+}]_i$ dependence of the gating of AdA-liganded channels, a saturating concentration (100 nM) of AdA was used as the ligand in the presence of various $[Ca^{2+}]_i$. The P_o of the channel activated by 100 nM AdA also varied with $[Ca^{2+}]_i$ in a biphasic manner (Fig. 3). At $[Ca^{2+}]_i < 1$ μM, increases in $[Ca^{2+}]_i$ enhanced the channel P_o. Between 1 and 20 μM $[Ca^{2+}]_i$, the channel P_o remained high (~0.8). As $[Ca^{2+}]_i$ increased beyond 20 μM, P_o decreased precipitously. This $[Ca^{2+}]_i$ dependence of the AdA-liganded *X*-InsP$_3$R-1 was essentially identical to that of the channel activated by saturating concentrations of InsP$_3$ (Mak et al., 1998). The results were well fitted by a biphasic Hill equation:

$$P_o = P_{max}[1 + (K_{act}/[Ca^{2+}]_i)^{H_{act}}]^{-1} [1 + ([Ca^{2+}]_i/K_{inh})^{H_{inh}}]^{-1}. \quad (2)$$

The Hill equation parameters—maximum P_o (P_{max}), half-maximal activating $[Ca^{2+}]_i$ (K_{act}), activation Hill coefficient (H_{act}), half-maximal inhibitory $[Ca^{2+}]_i$ (K_{inh}), and inhibition Hill coefficient (H_{inh})—for the AdA-liganded channel were all very similar to those for the InsP$_3$-liganded channel (Table I, A and B). The identical P_{max} indicates that InsP$_3$ and AdA have similar efficacy in gating the channel in the presence of 0.5 mM free ATP.

TABLE I

Hill Equation Parameters of X-InsP$_3$R-1

	Ligand concentration	P_{max}	K_{act}	H_{act}	K_{inh}	H_{inh}
			nM		*μM*	
A	100 nM AdA	0.81 ± 0.03	200 ± 50	1.8 ± 0.3	45 ± 5	3.5 ± 0.4
B	10 μM InsP$_3$	0.81 ± 0.03	190 ± 20	1.9 ± 0.3	54 ± 6	3.9 ± 0.7
C	0.5 nM AdA	0.84 ± 0.03	250 ± 50	1.8 ± 0.3	8.9 ± 0.5	4.3 ± 0.7
D	33 nM InsP$_3$	0.81 ± 0.03	190 ± 20	1.9 ± 0.3	11.0 ± 1.5	3.9 ± 0.7
E	20 nM InsP$_3$	0.81 ± 0.03	190 ± 20	1.9 ± 0.3	0.21 ± 0.04	3.9 ± 0.7
F	10 μM InsP$_3$	0.79 ± 0.02	420 ± 40	2.2 ± 0.3	110 ± 10	4.0 ± 0.7
G	33 nM InsP$_3$	0.80 ± 0.05	540 ± 70	2.0 ± 0.3	1.4 ± 0.2	3.5 ± 0.7
H	100 nM AdA	0.43 ± 0.03	400 ± 50	2.4 ± 0.3	130 ± 10	4.0 ± 0.7
I	20 nM AdA	0.44 ± 0.03	440 ± 40	2.6 ± 0.6	9 ± 2	4.0 ± 0.7

Parameters for the biphasic Hill equations (Eq. 2) that fit the $[Ca^{2+}]_i$ dependence of the P_o of *X*-InsP$_3$R-1 channel under various experimental conditions.

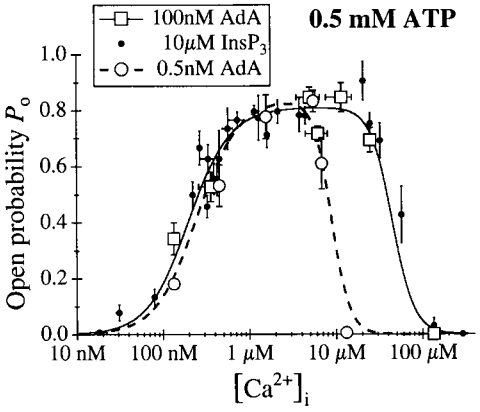

FIGURE 3. $[Ca^{2+}]_i$ dependence of the P_o of the *X*-$InsP_3R$-1 channel in the presence of 0.5 mM ATP, activated by AdA or $InsP_3$ (Mak and Foskett, 1998). The solid and dashed curves are theoretical fits by the Hill equation (Eq. 2) of the P_o data from [AdA] = 100 nM and 0.5 nM, respectively.

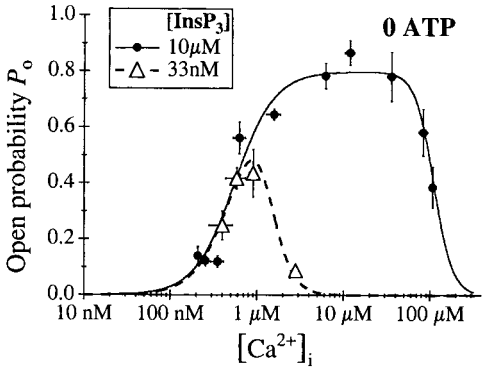

FIGURE 4. $[Ca^{2+}]_i$ dependence of the P_o of the *X*-$InsP_3R$-1 channel in the absence of ATP, activated by saturating (10 μM) or subsaturating (33 nM) concentrations of $InsP_3$. The solid and dashed curves are theoretical fits by the Hill equation (Eq. 2) of the P_o data.

The broad biphasic P_o versus $[Ca^{2+}]_i$ curve of the AdA-liganded *X*-$InsP_3R$-1 channel remained the same when the concentration of AdA was reduced from 100 to 5 nM (data not shown). However, when the concentration of AdA was further decreased to 0.5 nM, the channel exhibited a higher sensitivity to Ca^{2+} inhibition, with K_{inh} reduced, but H_{inh} unaltered (Table I C). The $[Ca^{2+}]_i$ dependence of the activation of the channel and the P_{max} were not significantly affected by the concentration of AdA (Fig. 3). AdA appears to activate the $InsP_3R$ channel by reducing the affinity of the Ca^{2+} inhibition site, which is reminiscent of the tuning of Ca^{2+} inhibition of the channel by $InsP_3$ (Mak et al., 1998). Thus, the mechanism by which ligand binding activates the channel (elevation of K_{inh}) is similar for both AdA and $InsP_3$. The value of K_{inh} of the channel activated by 0.5 nM AdA lies between those activated by 20 and 33 nM $InsP_3$ (Table I, D–E; Mak et al., 1998). Thus, in the presence of 0.5 mM ATP, AdA activates the *X*-$InsP_3R$-1 channel in the same manner with a similar efficacy as $InsP_3$, but AdA is ~60 times more potent than $InsP_3$.

$InsP_3$-liganded X-$InsP_3R$-1 Channel Gating in the Absence of ATP

Part of the molecular structure of AdA is analogous to that of $InsP_3$: AdA has a glucose moiety with a 3″,4″-bisphosphate/2″-hydroxyl motif that is structurally similar to the 4,5-bisphosphate/6-hydroxyl motif of $InsP_3$ (Hotoda et al., 1999), and the 2′-phosphoryl group in the ribose ring of AdA is probably in an analogous position as the 1-phosphoryl group in $InsP_3$ (Wilcox et al., 1995). However, the rest of the AdA molecular structure is very different from that of $InsP_3$ (Fig. 1). In particular, AdA has an adenosine 2′-phosphate moiety not present in $InsP_3$. An interaction between the adenine structure in AdA and unknown site(s) in the $InsP_3R$ has been suggested to contribute to the high potency of AdA as an agonist of the $InsP_3R$ (Hotoda et al., 1999).

The sequences of the regulatory domains of all $InsP_3R$ isoforms include putative ATP-binding site(s) (Mikoshiba, 1993). ATP was shown to bind to the $InsP_3R$ and regulate $InsP_3R$-mediated Ca^{2+} release and $InsP_3R$ single-channel gating (see INTRODUCTION). Because ATP and AdA share a common adenine moiety (Fig. 1), we reasoned that an ATP binding site(s) in the $InsP_3R$ structure might interact with the adenine moiety in AdA to promote high affinity binding of AdA to the channel. Such a mechanism suggests that ATP might function as an antagonist, competing with AdA for the same binding site in the $InsP_3R$. A prediction from this model is that the affinity of the channel for AdA would be increased in the absence of cytoplasmic free ATP. To test this hypothesis, we examined the activities of the channel in the absence of ATP, using either AdA or $InsP_3$ to stimulate gating.

We first examined the effects of $InsP_3$. In the absence of cytoplasmic free ATP, the channel conductance and gating properties activated by a saturating concentration of $InsP_3$ (10 μM) were identical to those of the channel activated in the presence of 0.5 mM ATP (Fig. 2 B). The $[Ca^{2+}]_i$ dependence of the channel P_o (Fig. 4) remained well characterized by a biphasic Hill equation (Eq. 2). The channel was fully activated in 2 μM < $[Ca^{2+}]_i$ < 50 μM with a P_{max} of 0.8. Whereas H_{act} and H_{inh} were similar in either the presence or absence of free ATP, the $InsP_3$-liganded channel in 0 ATP was less sensitive to Ca^{2+} activation and to Ca^{2+} inhibition (Fig. 5 A), with twofold increases in both K_{act} and K_{inh} (comparing Table I, F and B).

The biphasic $[Ca^{2+}]_i$ dependence of $InsP_3$-liganded channel gating in the absence of ATP remained unchanged when the concentration of $InsP_3$ was decreased from 10 μM to 100 nM (data not shown). A further reduction of the concentration of $InsP_3$ to 33 nM

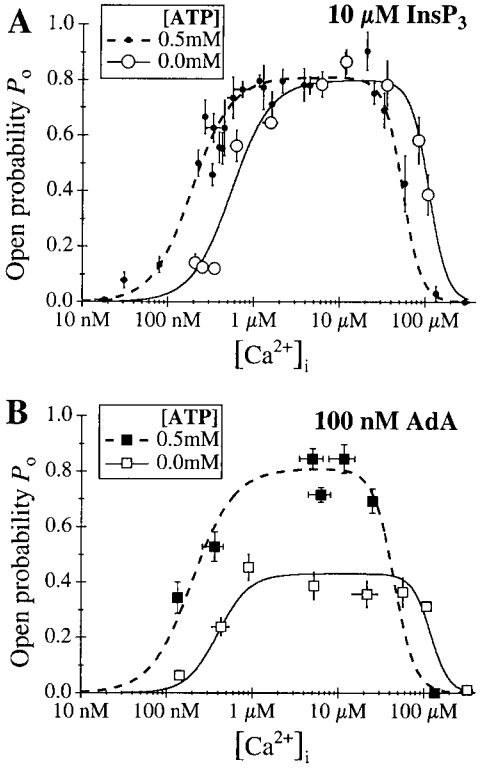

FIGURE 5. $[Ca^{2+}]_i$ dependence of the P_o of the *X*-$InsP_3R$-1 channel activated by saturating concentrations of ligands in the presence or absence of ATP. (A) 10 μM $InsP_3$; (B) 100 nM AdA. The solid and dashed curves are theoretical fits by the Hill equation (Eq. 2) of the data in 0 or 0.5 mM of ATP, respectively.

caused the channel to exhibit a higher sensitivity to Ca^{2+} inhibition (Fig. 4). The $[Ca^{2+}]_i$ dependence of the channel P_o activated by 33 nM $InsP_3$ in the absence of ATP was fitted by the biphasic Hill equation (Eq. 2) with K_{inh} reduced from 110 to 1.4 μM, while the other parameters H_{inh}, K_{act}, H_{act}, and P_{max} remained essentially unchanged (Table I G). Thus, $InsP_3$ regulation of *X*-$InsP_3R$-1 channel gating was similar in the presence or absence of ATP, with comparable efficacy and functional affinity in both cases.

AdA-liganded X-InsP₃R-1 Channel Gating in the Absence of ATP

We next examined the effects of AdA. The conductance properties of the *X*-$InsP_3R$-1 channel activated by a saturating concentration (100 nM) of AdA were indistinguishable in either the presence or absence of ATP (Fig. 2). In contrast, gating of the AdA-liganded channel in the absence of ATP was dramatically different from that of the $InsP_3$-liganded channel. Whereas the $InsP_3$-liganded channel exhibited $P_{max} \approx 0.8$ at $[Ca^{2+}]_i > 2$ μM, the P_{max} of the AdA-liganded channel was only 0.4 (Figs. 5 B and 6). Instead of staying open most of the time with only brief closings like the $InsP_3$-liganded channel, the AdA-liganded channel had substantially

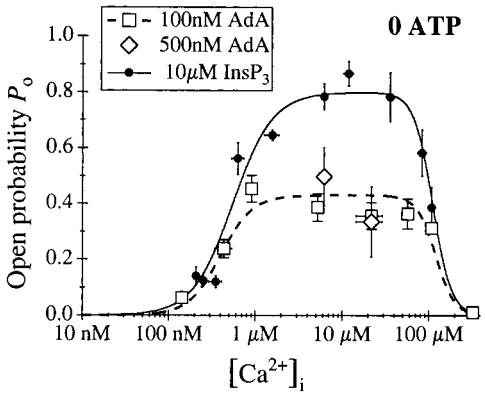

FIGURE 6. $[Ca^{2+}]_i$ dependence of the P_o of the *X*-$InsP_3R$-1 channel activated by AdA or $InsP_3$ in the absence of ATP. The solid and dashed curves are theoretical fits by the Hill equation (Eq. 2) of the P_o data from $[InsP_3]$ = 10 μM and [AdA] = 100 nM, respectively.

shorter channel openings (Fig. 2 B). Similar channel gating characterized by short openings (Fig. 2 B) and P_{max} of ~0.4 (Fig. 6) was also observed in suprasaturating concentrations (500 nM) of AdA. Therefore, the altered gating kinetics of the AdA-liganded channel observed in the absence of ATP was not due to insufficient channel activation by subsaturating concentrations of AdA.

The $[Ca^{2+}]_i$ dependence of the AdA-liganded channel P_o in the absence of ATP (Figs. 5 A and 6) was well fitted by the biphasic Hill equation (Eq. 2) with K_{act}, H_{act}, K_{inh}, and H_{inh} comparable with those for the channel activated by $InsP_3$, but with a P_{max} decreased to ~0.4 (Table I H). Therefore, in the absence of ATP, the affinities (K_{act} and K_{inh}) of the activating and inhibitory Ca^{2+}-binding sites and their levels of cooperativity (H_{act}

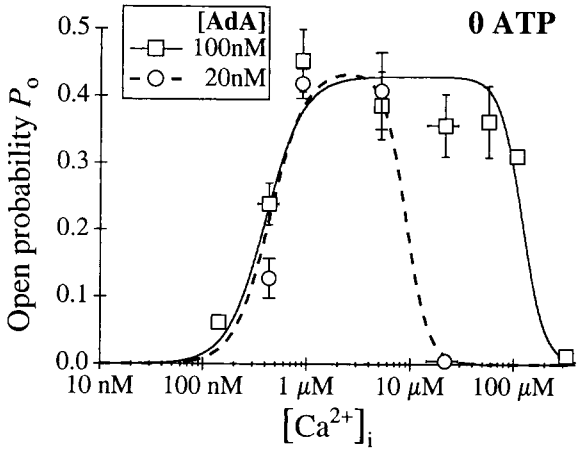

FIGURE 7. $[Ca^{2+}]_i$ dependence of the P_o of the *X*-$InsP_3R$-1 channel in the absence of ATP, activated by saturating (100 nM) or subsaturating (20 nM) concentrations of AdA. The solid and dashed curves are theoretical fits by the Hill equation (Eq. 2) of the P_o data. Note that the scale of the P_o axis is different from that in the previous P_o versus $[Ca^{2+}]_i$ graphs.

and H_{inh}) of the AdA and $InsP_3$-liganded *X*-$InsP_3R$-1 channels were similar, but the maximal level of channel activity induced by AdA in the absence of ATP was only about half that activated by $InsP_3$ at all $[Ca^{2+}]_i$. In other words, in the absence of free ATP, AdA was less efficacious than $InsP_3$ in activating channel gating, acting instead as a partial agonist.

When the concentration of AdA was reduced from 100 to 20 nM in the absence of ATP, the channel became more sensitive to Ca^{2+} inhibition (Fig. 7), with only K_{inh} reduced while the other Hill equation parameters remained similar to those observed in 100 nM AdA (Table I). Thus, despite the lower P_{max} value observed for the channel activated by AdA in the absence of ATP, the channel was still activated by ligand tuning of its sensitivity to Ca^{2+} inhibition, as it was when it was activated by $InsP_3$ (Mak et al., 1998; Fig. 4), or by AdA in 0.5 mM ATP (Fig. 3).

Of note, the value of K_{inh} for the channel activated by 20 nM AdA in the absence of ATP lay between those values for channels activated by 33 and 100 nM $InsP_3$. Thus, in the absence of ATP, AdA was only 1.5–5 times more potent than $InsP_3$ in activating the channel, whereas it was ~60 times more potent in the presence of 0.5 mM ATP.

In summary, the affinities of the activating and inhibitory Ca^{2+}-binding sites (K_{act} and K_{inh}) of the $InsP_3$-liganded channels were the only parameters affected by the presence or absence of ATP (Fig. 5 A). In contrast, ATP regulates not only the affinities of the Ca^{2+}-binding sites, but also the level of maximum activity of the AdA-liganded channel (Fig. 5 B) as well as the potency of AdA to activate the channel. Thus, the presence or absence of ATP affects all regulation parameters of the AdA-liganded channel except the level of cooperativity of the Ca^{2+}-binding sites. In addition, these results demonstrate that the high affinity of AdA is not conferred by its interaction with ATP-binding sites in the channel sequence, in contrast to our working hypothesis.

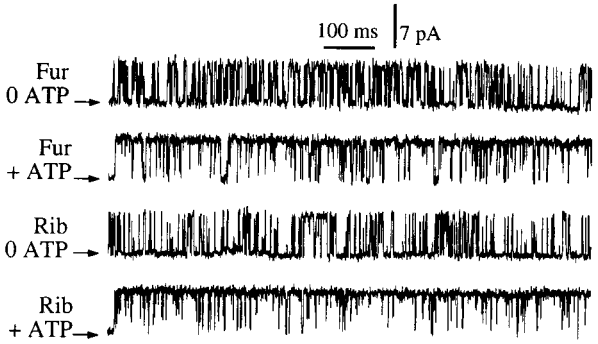

FIGURE 8. Typical single-channel current traces of the *X*-$InsP_3R$-1 activated by 10 μM Fur or Rib. In 0.5 mM ATP (+ ATP), $[Ca^{2+}]_i$ = 5.0 μM. In the absence of ATP (0 ATP), $[Ca^{2+}]_i$ = 6.2 μM. The arrows indicate the closed channel current levels.

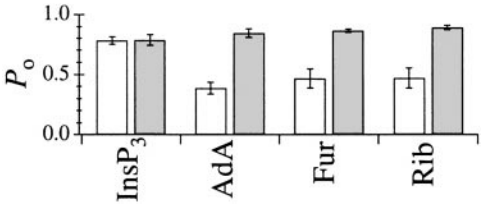

FIGURE 9. P_o of the *X*-$InsP_3R$-1 channel in optimal $[Ca^{2+}]_i$ (4.4–6.2 μM) and saturating concentrations of various ligands in 0 (white bars) and 0.5 mM (shaded bars) ATP.

Properties of the X-InsP₃R-1 Channel Activated by Rib and Fur

Because AdA and $InsP_3$ had distinct effects on the gating properties of the $InsP_3R$ when the channel was stimulated in the absence of ATP, we speculated that the distinct molecular structures of the two ligands conferred unique ATP-dependent gating properties. To determine the molecular structural determinants in the activating ligand that influence the gating properties of the channel, we investigated the effects of Rib and Fur, structural analogues of AdA that lack the adenine moiety found in AdA (Fig. 1). In previous studies, these analogues of AdA were found to stimulate $InsP_3$-mediated Ca^{2+} release with an apparent affinity that was significantly lower than that of AdA but similar to that of $InsP_3$ (Marchant et al., 1997; Shuto et al., 1998).

In optimal conditions, with $[Ca^{2+}]_i$ between 4.4 and 6.2 μM and in the presence of saturating concentrations (10 μM) of Rib or Fur, the channels exhibited inactivation kinetics and conductance and gating properties (Fig. 8) that were indistinguishable from those observed when the channels were activated by AdA, in either the absence or presence (0.5 mM) of ATP (Fig. 2). Whereas $InsP_3$-liganded channels exhibited P_{max} of ~0.8 in both 0 and 0.5 mM ATP, channels activated by AdA, Fur, or Rib only exhibited this high P_{max} in the presence of 0.5 mM ATP. In the absence of ATP, the *X*-$InsP_3R$-1 channel activated by AdA, Fur, or Rib had a significantly ($P < 0.01$) lower $P_{max} \approx 0.4$ (Fig. 9). Thus, the responses of the channel to saturating concentrations of Fur or Rib were clearly similar to that for AdA and different from those for $InsP_3$.

Closed Channel Dwell Time Distributions of X-InsP₃R-1 Channel Activated by Various Ligands

To elucidate the kinetic features associated with the regulation of *X*-$InsP_3R$-1 channel gating, we studied in detail the mean open and closed channel durations ($\langle\tau^o\rangle$ and $\langle\tau^c\rangle$, respectively) under various experimental conditions in the presence of different ligands. Furthermore, dwell time histogram analyses were performed on single-channel current records of channels activated by saturating concentrations of AdA (100 nM)

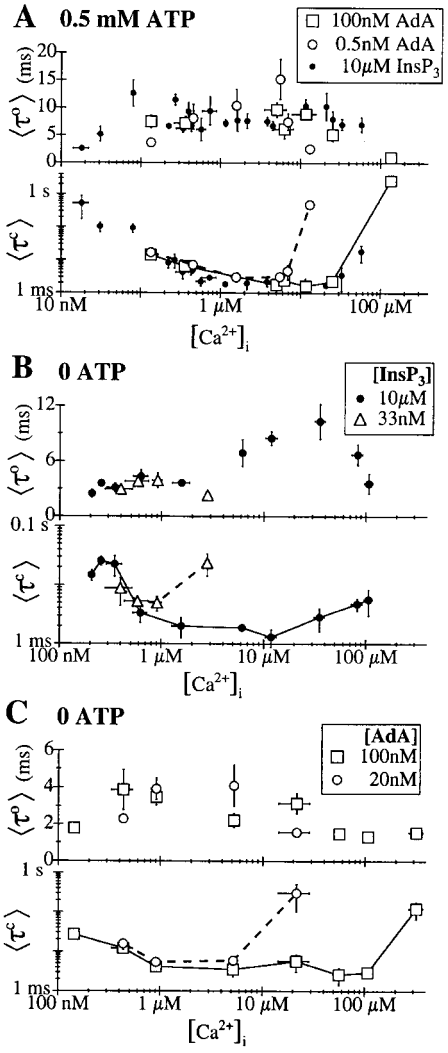

FIGURE 10. $[Ca^{2+}]_i$ dependencies of the mean open ($\langle\tau^o\rangle$) and closed ($\langle\tau^c\rangle$) dwell times of the *X*-InsP$_3$R-1 channel. In the $\langle\tau^c\rangle$ graphs, data points from the same experimental conditions are connected with solid or dashed lines for clarity. (A) Channel activated by AdA or InsP$_3$ (Mak and Foskett, 1998), in 0.5 mM ATP. (B) Channel activated by saturating (10 μM) or subsaturating (33 nM) concentrations of InsP$_3$ in the absence of ATP. (C) Channel activated by saturating (100 nM) or subsaturating (20 nM) concentrations of AdA in the absence of ATP.

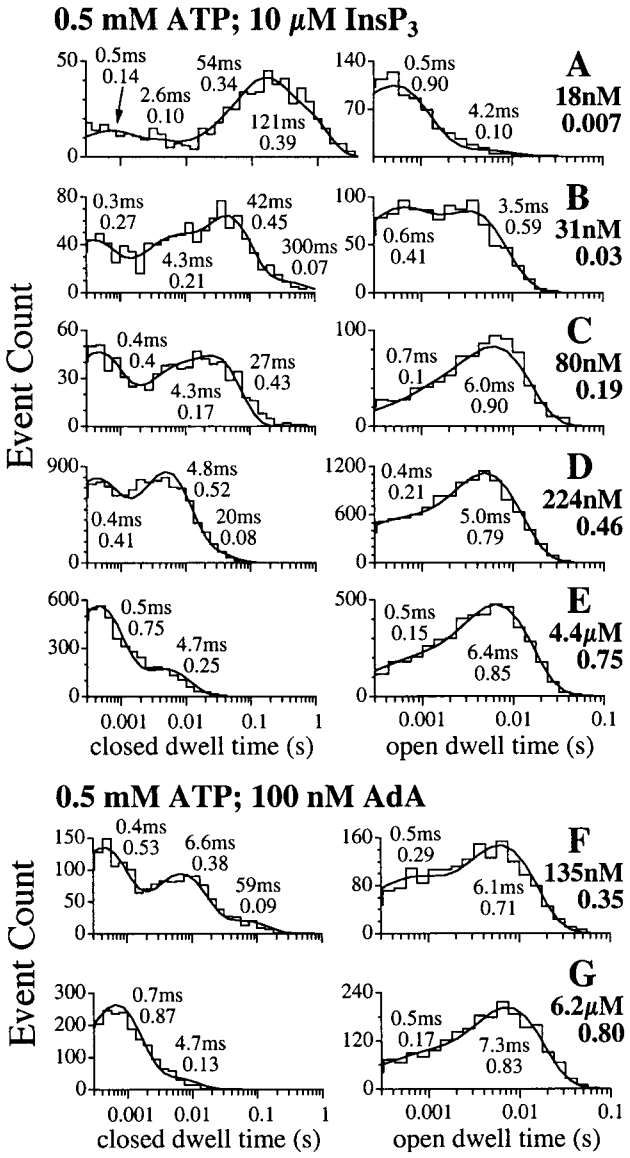

FIGURE 11. Open and closed dwell time histograms of the *X*-InsP$_3$R-1 channel in 0.5 mM ATP and various $[Ca^{2+}]_i$, activated by saturating concentrations of InsP$_3$ (10 μM) or AdA (100 nM). The smooth curves are the pdf. The time constant and relative weight of each exponential component of the pdf are tabulated next to the corresponding peak in the curves. $[Ca^{2+}]_i$ used in each of the analyzed experiments and its P_o are tabulated next to the corresponding graphs.

or InsP$_3$ (10 μM), in the presence or absence of ATP, and in various $[Ca^{2+}]_i$, except when such analyses were precluded by Ca^{2+} inhibition at high $[Ca^{2+}]_i$ and channel inactivation (Mak and Foskett, 1997).

In general, under all conditions examined (activation by AdA or InsP$_3$, in the presence or absence of ATP), the $[Ca^{2+}]_i$ dependence of the channel P_o mainly resided in a $[Ca^{2+}]_i$ dependence of $\langle\tau^c\rangle$ (Mak et al., 1998; Fig. 10). The increase in P_o due to Ca^{2+} activation in the low $[Ca^{2+}]_i$ range (<1 or 2 μM, in the presence or absence of ATP, respectively) was mostly caused by a decrease in $\langle\tau^c\rangle$ with increases in $[Ca^{2+}]_i$. $\langle\tau^c\rangle$ stayed within a narrow range (1 to 5 ms) when P_o remained at maximum level in higher, optimal $[Ca^{2+}]_i$. The precipitous decrease in P_o at higher $[Ca^{2+}]_i$ due to Ca^{2+} inhibition was mostly the result of a dramatic rise in $\langle\tau^c\rangle$ as $[Ca^{2+}]_i$ increased. The increase in the sensitivity of the channel to Ca^{2+} inhibition observed in the presence of subsaturating concentrations of either ligand (AdA or InsP$_3$) was reflected in an onset of the rise in $\langle\tau^c\rangle$ at lower $[Ca^{2+}]_i$.

The closed dwell time histograms of the *X*-InsP$_3$R-1 channel revealed that it had at least four distinguishable closed kinetic states with time constants τ^c >100 ms, 20–

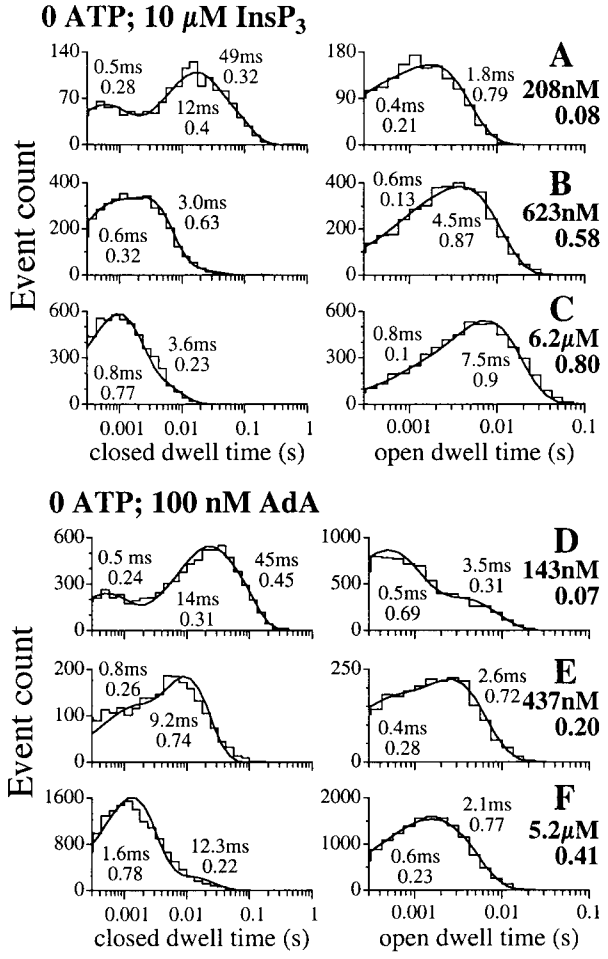

FIGURE 12. Open and closed dwell time histograms of the *X*-InsP$_3$R-1 channel in the absence of ATP and various $[Ca^{2+}]_i$, activated by saturating concentrations of InsP$_3$ (10 μM) or AdA (100 nM). The smooth curves are the pdf. The time constant and relative weight of each exponential component of the pdf are tabulated next to the corresponding peak in the curves. $[Ca^{2+}]_i$ used in each of the analyzed experiments and its P_o are tabulated next to the corresponding graphs.

60 ms, 2–10 ms, and <1 ms, respectively (Figs. 11 and 12). The decrease in $\langle\tau^c\rangle$ associated with Ca^{2+} activation of InsP$_3$-liganded channels in 0.5 mM ATP was caused by sequential destabilization and, therefore, reduction of the relative weights, of the three longer closed kinetic states, until the shortest closed kinetic state with $\tau^c < 1$ ms became dominant in $[Ca^{2+}]_i > 1$ μM (Fig. 11, A–E). Reduction of τ^c of the longer closed kinetic states also contributed, to a lesser extent, to the decrease in $\langle\tau^c\rangle$.

As suggested by their essentially identical $[Ca^{2+}]_i$ dependencies of the P_o (Fig. 3) and $\langle\tau^c\rangle$ (Fig. 10 A) of channels activated in 0.5 mM ATP by either AdA or InsP$_3$, the closed channel dwell time distributions of the channels activated by either ligand in 0.5 mM ATP were very similar (Fig. 11). Although the sensitivity of the channels to Ca^{2+} activation was diminished in the absence of ATP, the closed dwell time distributions of InsP$_3$-liganded channels in the absence of ATP resembled those in the presence of 0.5 mM ATP when compared at $[Ca^{2+}]_i$ that gave comparable channel P_o (compare Fig. 12, A–C, with Fig. 11, C–E).

Interestingly, although the gating kinetics of the InsP$_3$R channel activated by AdA in the absence of ATP were very different from those of channels activated by AdA in 0.5 mM ATP or activated by InsP$_3$ (Fig. 2), Ca^{2+} activation of the AdA-liganded InsP$_3$R in the absence of ATP was still caused by destabilization of the longer closed kinetic states (Fig. 12, D–F), although the closed channel time constants were generally longer than in other conditions.

Open Channel Dwell Time Distributions of X-InsP$_3$R-1 Channels Activated by Various Ligands

The mean open channel duration ($\langle\tau^o\rangle$) of the *X*-InsP$_3$R-1 channel activated by saturating concentrations of InsP$_3$ in 0.5 mM ATP remained within a narrow range, between 5 and 15 ms, over a wide range of $[Ca^{2+}]_i$ (50 nM–50 μM; Fig. 10 A). $\langle\tau^o\rangle$ dropped below 5 ms at very low or very high $[Ca^{2+}]_i$. In subsaturating concentrations of InsP$_3$, $\langle\tau^o\rangle$ dropped below 5 ms at lower $[Ca^{2+}]_i$ (Mak et al., 1998). This $[Ca^{2+}]_i$ dependence of $\langle\tau^o\rangle$ was mirrored in AdA-liganded channels in 0.5 mM ATP (Fig. 10 A). A similar $[Ca^{2+}]_i$ dependence of $\langle\tau^o\rangle$ was also observed in InsP$_3$-liganded channels in 0 ATP, except that $\langle\tau^o\rangle$ was >5 ms for $[Ca^{2+}]_i$ between 300 nM and 100 μM in saturating concentrations of InsP$_3$ because of the change in $[Ca^{2+}]_i$ sensitivity of the channel in the absence of ATP (Fig. 10 B).

In contrast, a very different $[Ca^{2+}]_i$ dependence was observed for $\langle\tau^o\rangle$ of the AdA-liganded channel in 0 ATP. $\langle\tau^o\rangle$ never rose above 5 ms over the entire wide range of $[Ca^{2+}]_i$ examined (Fig. 10 C). This reduced $\langle\tau^o\rangle$ accounted for the distinct channel gating kinetics of the InsP$_3$R activated by AdA in 0 ATP. Thus, a typical opening event of the channel activated by AdA in the absence of ATP was significantly shorter than a typical opening event of the channel under other activating conditions examined. This was the major factor contributing to the low value of P_{max} for the AdA-liganded channel in 0 ATP.

Open dwell time histograms of the fully activated *X*-InsP$_3$R-1 channel generally contained two exponential components, corresponding to at least two distinguishable open kinetic states (Figs. 11 and 12). Over most $[Ca^{2+}]_i$ in which the channel $\langle\tau^o\rangle$ remained high, the long open kinetic state was the dominant one. At very low $[Ca^{2+}]_i$, $\langle\tau^o\rangle$ of the channel was shorter because of either the sharp reduction in the relative weight of the long open kinetic state in favor of the short one (for InsP$_3$-liganded channel in 0.5 mM ATP; Fig. 11, A and B; and AdA-liganded channel in 0 ATP; Fig 12 D), or the

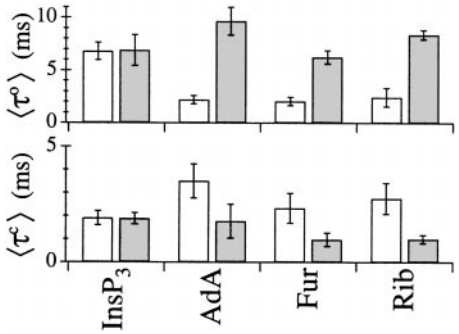

FIGURE 13. $\langle\tau^c\rangle$ and $\langle\tau^o\rangle$ of *X*-InsP$_3$R-1 channels in optimal $[Ca^{2+}]_i$ (4.4–6.2 μM) and saturating concentrations of various ligands in 0 (white bars) and 0.5 mM (shaded bars) ATP.

reduction of the time constant of the long open kinetic state (for InsP$_3$-liganded channel in 0 ATP; Fig. 12 A).

The time constant τ^o of the dominating long open kinetic state was 5–8 ms for all experimental conditions in which the channel had P_{max} of 0.8: channels in 0.5 mM ATP activated by InsP$_3$ (Fig. 11, C–E) or AdA (Fig. 11, F and G), and InsP$_3$-liganded channels in 0 ATP (Fig. 12, B and C). In contrast, τ^o of the dominating long open kinetic state was only ~2 ms for AdA-liganded channel in 0 ATP with P_{max} of 0.4 (Fig. 12, E and F).

Comparison of $\langle\tau^o\rangle$ and $\langle\tau^c\rangle$ of the InsP$_3$R channel in saturating concentrations of various ligands (Fig. 13) clearly indicated that the channel optimally activated by Rib or Fur exhibited the same gating kinetics as AdA-liganded channels, characterized by having a significantly shorter $\langle\tau^o\rangle$ and a longer $\langle\tau^c\rangle$ in the absence of ATP than in the presence of ATP. In contrast, InsP$_3$-liganded channels exhibited the same $\langle\tau^o\rangle$ and $\langle\tau^c\rangle$ under both conditions.

DISCUSSION

Since its discovery as a potent, metabolically stable agonist of the InsP$_3$R, AdA has been used in studies of the InsP$_3$R and its regulation and in studies that examined intracellular Ca^{2+} release in cells (see INTRODUCTION). Our study represents the first investigation of the single-channel properties of the InsP$_3$R channel in its native membrane environment activated by AdA and its analogues.

ATP-dependent Differences in InsP$_3$R Gating Activated by InsP$_3$ and AdA

The major finding in our study is that AdA activates the InsP$_3$R channel with distinct properties depending on the presence or absence of ATP. In the presence of 0.5 mM cytoplasmic free ATP, the endogenous *Xenopus* type 1 InsP$_3$R channel activated by AdA was indistinguishable from the InsP$_3$-liganded channel. The conductance properties, channel gating properties, biphasic Ca^{2+} activation and inhibition, and tuning of the sensitivity to Ca^{2+} inhibition by the agonist concentration were identical for InsP$_3$- and AdA-liganded InsP$_3$R. The efficacy of the two ligands (i.e., P_{max} of the channel that the two ligands can elicit) was also comparable. However, the potency of AdA as an agonist to reduce the sensitivity of the channel to Ca^{2+} inhibition (i.e., increasing K_{inh}) was ~60 times that of InsP$_3$. This figure agrees well with the affinity of the channel for AdA determined by binding and Ca^{2+} release assays (Takahashi et al., 1994; Hirota et al., 1995; Murphy et al., 1997). Thus, in the presence of ATP, the sole distinguishing feature between channels activated by the two ligands is the higher functional affinity of the channel for AdA compared with InsP$_3$. Therefore, the liganded channel in the presence of ATP must attain comparable structural conformations that result in kinetically indistinguishable gating and regulatory behaviors, independent of the nature of the specific ligand.

On the other hand, the nature of the ligand was critically important in determining the kinetic and regulatory properties of the channel when ATP was absent. ATP has been previously shown to stimulate the activities of the InsP$_3$-liganded type 1 InsP$_3$R channels (Ferris et al., 1990; Iino, 1991; Bezprozvanny and Ehrlich, 1993; Missiaen et al., 1997; Landolfi et al., 1998). In a detailed study that used the same experimental conditions as those employed in the present study, ATP was demonstrated to enhance the sensitivity (lowering K_{act}) of the type 1 InsP$_3$R channels to Ca^{2+} activation (Mak et al., 1999). New data obtained in this study indicates that ATP also increases the sensitivity of the channel to Ca^{2+} inhibition (lowering K_{inh}). However, the P_{max} and the gating kinetics ($\langle\tau^o\rangle$ and $\langle\tau^c\rangle$) of optimally activated InsP$_3$-liganded channels are not affected by ATP (Mak et al., 1999; and this study). Furthermore, the affinity of the channel for InsP$_3$ is also not substantially affected by ATP (up to 0.5 mM; this study).

In marked contrast, when the channels were activated by AdA, the presence or absence of ATP (0 vs. 0.5 mM) profoundly affected the P_{max} of the channel and the gating kinetics, as well as the potency of AdA to activate the channel. Although ATP enhanced the sensitivities of the AdA-liganded *X*-InsP$_3$R-1 channel to both Ca^{2+} activation and inhibition to the same extent as for InsP$_3$-liganded channels, channels activated by AdA in the absence of ATP had a decreased P_{max}, altered gating kinetics (mainly decreased $\langle\tau^o\rangle$), and diminished functional affinity for AdA. Thus, in the absence of ATP, several features distinguish channels activated by either InsP$_3$ or AdA. Both the efficacy and apparent affinity of AdA become significantly reduced in the absence of ATP. Whereas AdA is a full agonist in the presence of ATP, it is only a partial agonist in its absence. InsP$_3$, on the other hand, is a full agonist in either the presence or absence of free ATP. Therefore, the InsP$_3$-liganded and AdA-

liganded channels in the absence of ATP must attain distinct structural conformations that result in kinetically distinguishable gating and regulatory behaviors.

Molecular Structural Basis of Interactions between the $InsP_3R$ and Its Agonists

Based on comparisons of the molecular structures of analogues of $InsP_3$ (Irvine et al., 1984) and AdA (Takahashi et al., 1994; Wilcox et al., 1995; Marchant et al., 1997; Shuto et al., 1998; Beecroft et al., 1999; Hotoda et al., 1999) that activate Ca^{2+} release through the $InsP_3R$ channel, and on our study of the single-channel activities of $InsP_3R$ activated by AdA and its analogues under various conditions, three structural elements can be identified that contribute to the interactions between the channel and its agonists.

First, AdA and most of its structural analogues that activate the $InsP_3R$ with high potency have a glucose moiety with a 3′′,4′′-bisphosphate/2′′-hydroxyl motif (Fig. 1) that is structurally similar to the 4,5-bisphosphate/6-hydroxyl motif of $InsP_3$ and its analogues that activate the $InsP_3R$. Therefore, interactions between this structural element and the $InsP_3$ binding site of the $InsP_3R$ are necessary for activation of $InsP_3R$ channel activity.

Second, although many structural analogues of AdA also bind and activate the $InsP_3R$, their binding affinities ($1/K_d$) and functional potencies ($1/EC_{50}$) for the channel are all significantly lower than those of AdA. AdA has an adenosine 2′-phosphate moiety (Fig. 1) not present in any of its analogues. Thus, it has been proposed that interactions between this second structural element and the $InsP_3R$ enhance the affinity of the channel for AdA (Hotoda et al., 1999). As AdA and ATP share a common adenine moiety in their molecular structures (Fig. 1), we initially considered that some interaction of AdA with an ATP binding site(s) in the $InsP_3R$ might contribute to high affinity binding. However, our single-channel results provide no evidence for ATP being an antagonist competing with AdA for the same binding site(s) in the $InsP_3R$, as the presence of cytoplasmic free ATP enhanced rather than reduced the functional potency of AdA to activate channel gating (Figs. 3 and 7). Therefore, we conclude that ATP and AdA must bind to distinct sites in the $InsP_3R$. In support of this conclusion, peptides containing putative ATP-binding sequences in the $InsP_3R$ bind ATP but not AdA (Maes et al., 1999), and the NH_2-terminal ligand-binding domain of the $InsP_3R$ itself contains the site(s) responsible for high affinity binding of AdA to the receptor (Glouchankova et al., 2000).

The third structural element contributing to AdA interaction with the $InsP_3R$ is the 2′-phosphoryl group in the ribose ring of AdA, Rib, and Fur. This element is probably in an analogous position as the 1-phosphoryl group in $InsP_3$ (Wilcox et al., 1995), although it has a different physical location relative to the 3′′,4′′-bisphosphate/2′′-hydroxyl motif in AdA and its analogues compared with the 1-phosphoryl group in $InsP_3$ relative to the 4,5-bisphosphate/6-hydroxyl motif (Hotoda et al., 1999). Interaction between this element and the $InsP_3R$ is necessary for the activation of the $InsP_3R$ by its agonists (Irvine et al., 1984)

Molecular Model for Allosteric Effects of ATP on Ligand Gating of $InsP_3R$

How can we account for the dramatic effects of ATP on the functional interaction of AdA with the channel? How is it that, in the presence of ATP, AdA elicited identical channel activation and gating as $InsP_3$ but with a much higher potency, whereas in the absence of ATP, AdA had only approximately twofold higher potency than $InsP_3$ and could only activate the $InsP_3R$ half as efficaciously as $InsP_3$?

As discussed above, there is no evidence for a direct interaction of AdA and ATP with the same sites in the $InsP_3R$. Therefore, the effects of ATP on the functional interaction of AdA with the receptor are likely mediated by allosteric interactions. We suggest that ATP binds to a site in the $InsP_3R$ different from the NH_2-terminal ligand-binding site, likely within the regulatory domain that links the ligand-binding domain to the channel domain. Binding of ATP to this site produces an allosteric conformational change in the ligand-binding site that enhances the binding of AdA to the channel, as illustrated in Fig. 14. The model shown in Fig. 14 assumes that this enhanced binding of AdA to $InsP_3R$ is caused by interaction between the receptor and the adenine moiety in AdA (Hotoda et al., 1999), but it is possible that the enhanced functional affinity of AdA to the $InsP_3R$ in the presence of ATP is due to the adenine structure in AdA positioning the 2′-phosphoryl group in the ribose ring of AdA for a more optimal interaction with the receptor (Hotoda et al., 1999).

As shown in Fig. 14, the 1-phosphoryl group in $InsP_3$ interacts equally well with the conformations of the ligand-binding site of the $InsP_3R$ in either the presence or absence of ATP. This interaction elicits the same channel gating kinetics independent of ATP (Fig. 2). In the presence of ATP, the 2′-phosphoryl group in AdA, Rib, or Fur can bind to the same phosphoryl group-binding site in the receptor that $InsP_3$ interacts with, so that the channel gating kinetics evoked by AdA, Fur, and Rib are indistinguishable from those evoked by $InsP_3$ (Figs. 2 A and 8). Under these conditions, AdA has equal efficaciousness as a full agonist as $InsP_3$. In contrast, in the distinct conformation that the $InsP_3R$ assumes in the absence of ATP, the 2′-phosphoryl group in AdA, Fur, or Rib has a different interaction with the $InsP_3R$ ligand-binding site (possibly through an alternate phosphoryl group interacting site). When AdA is bound to the chan-

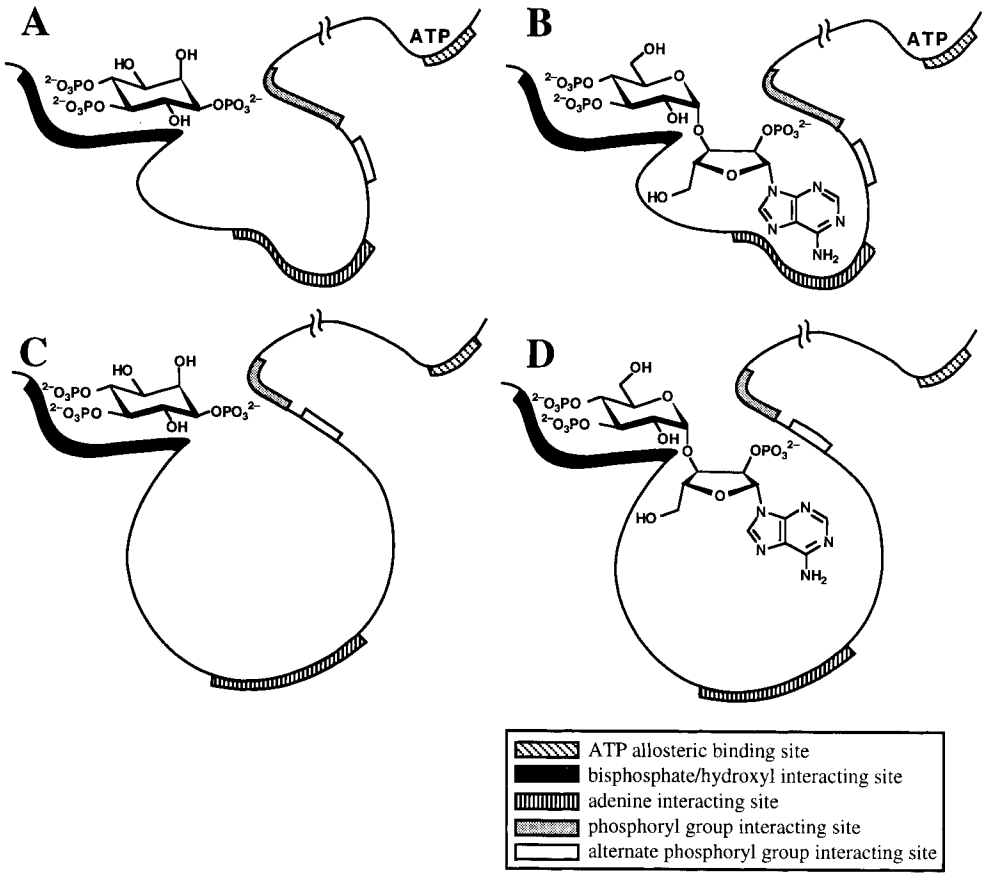

FIGURE 14. Schematic diagrams representing interactions between the *X*-InsP$_3$R-1 molecule and various ligands. (A) Interaction between *X*-InsP$_3$R-1 and InsP$_3$ in the presence of ATP. (B) Interaction between *X*-InsP$_3$R-1 and AdA in the presence of ATP. (C) Interaction of *X*-InsP$_3$R-1 and InsP$_3$ in the absence of ATP. (D) Interaction of *X*-InsP$_3$R-1 and AdA in the absence of ATP.

nel in this conformation, the channel gates differently (Figs. 2 B and 8) because the interaction is less able to stabilize the channel open state as when the channel is bound to InsP$_3$ or AdA in the presence of ATP. Therefore, AdA gates the channel less efficaciously, behaving as a partial agonist. The interaction between this element and the InsP$_3$R is not only necessary for the activation of the InsP$_3$R by its agonists, but also determines the gating kinetics of the activated channel.

The regulatory region of the InsP$_3$R, where ATP likely binds, has been regarded as a transduction region which links the NH_2-terminal ligand-binding domain to the gating machinery associated with the COOH-terminal channel pore region. Our results suggest that the regulatory region influences the properties of the ligand-binding domain as well as the coupling between ligand binding and channel gating. Binding of either ligand, InsP$_3$ or AdA, activates channel gating by destabilizing channel closed states (Mak et al., 1998). ATP activates the liganded channel also by destabilizing closed states, tuning the Ca^{2+} sensitivity of distinct activating Ca^{2+}-binding sites (Mak et al., 1999). Regulation of open channel states has not been previously implicated in the mechanisms by which InsP$_3$R channel gating is regulated by ligands, Ca^{2+}, and ATP (Mak et al., 1998; Mak et al., 1999; and this study). The present study has identified distinct channel open times as the major kinetic feature that accounts for the significant reduction in the efficacy of AdA as an agonist. This result now suggests that ligand binding plays a role in stabilizing channel open states, in addition to destabilizing closed kinetic states.

Relationship of Channel Gating to Kinetics of AdA-induced Ca^{2+} Release through the InsP$_3$R Observed in Xenopus Oocytes

Previous studies of AdA-induced intracellular Ca^{2+} release in *Xenopus* oocytes by confocal imaging (Marchant and Parker, 1998) or measurements of plasma membrane Ca^{2+}-activated Cl^- currents (DeLisle et al., 1997; Hartzell et al., 1997; Machaca and Hartzell, 1999) indicated that Ca^{2+} release through InsP$_3$R activated by AdA was qualitatively different from that activated by InsP$_3$. Our results demonstrate that the properties of the *X*-InsP$_3$R-1 channel activated by AdA are indistinguishable from those activated by InsP$_3$ in the presence of 0.5 mM cytoplasmic ATP. The profound effects of ATP on the AdA-liganded channels observed in this study were due to free ATP, as Mg^{2+} was not present. Thus, the distinct cytoplasmic calcium signals measured in oocytes activated by AdA may suggest that the level of free ATP in *Xenopus* oocyte cytoplasm was lower than 0.5 mM in

those studies. Total ATP content in cells is 4–8 mM, most of which is complexed with Mg^{2+} (Flatman, 1991). With 4 mM each of ATP and Mg^{2+}, free ATP is predicted to be ~0.35 mM; with 8 mM of each, free ATP is predicted to be ~0.5 mM. Thus, free ATP concentrations in the oocyte cytoplasm may realistically be expected to be <0.5 mM, as our results predict.

Nevertheless, some features of the calcium signals evoked by AdA in oocytes are consistent with a high affinity of the $InsP_3R$ for AdA, which our results suggest is dependent on the presence of ATP. The slower rate of propagation of calcium waves activated by AdA (Bird et al., 1999; Machaca and Hartzell, 1999) and the more spatially restricted calcium signals observed in the presence of AdA (Bird et al., 1999) were both interpreted to reflect a substantially reduced diffusion coefficient of AdA in the oocyte cytoplasm because of high affinity binding to the $InsP_3R$ (Machaca and Hartzell, 1999). Our study suggests that the affinity of the $InsP_3R$ for AdA is significantly higher than that for $InsP_3$ only in the presence of cytoplasmic free ATP (Figs. 3 and 7). Thus, the oocyte cytoplasm, although having a free ATP concentration <0.5 mM, must nevertheless contain a finite concentration of free ATP, as expected. Therefore, we conclude that the *Xenopus* oocytes have cytoplasmic free ATP concentrations between 0 and 0.5 mM.

Our results demonstrate that AdA may or may not elicit a similar response from the $InsP_3R$ as $InsP_3$, depending on the concentration of cytoplasmic free ATP. Without knowledge or control of the cytoplasmic free ATP concentration in experiments using AdA to investigate intracellular calcium signaling, AdA cannot be regarded simply as a nonmetabolizable, more potent substitute for $InsP_3$ as an agonist of the $InsP_3R$.

With this in mind, the single-channel gating kinetics of the *X*-$InsP_3R$-1 activated by AdA observed in our nuclear patch-clamp experiments can reasonably account for results obtained in the in vivo Ca^{2+} release studies. First, the rate of Ca^{2+} release in oocytes stimulated with a high concentration of AdA (~2 μM) was only half of that stimulated by high concentrations of $InsP_3$ (~20 μM; Machaca and Hartzell, 1999). This can be explained by our observation that P_{max} of the $InsP_3R$ channel activated by AdA was substantially lower than that activated by $InsP_3$ at the suboptimal ATP concentrations in the oocyte cytoplasm. Second, 5 nM AdA elicited a significantly slower rate of Ca^{2+} release than 2 μM AdA (Machaca and Hartzell, 1999), although both concentrations would have been predicted to be saturating for binding to the channel (Takahashi et al., 1994; Hirota et al., 1995; Murphy et al., 1997; and this study). Our patch-clamp experiments revealed that at suboptimal free ATP concentrations in the oocyte cytoplasm, the affinity of AdA for the channel is likely reduced, such that 5 nM AdA may become subsaturating and, therefore, elicit a significantly lower rate of Ca^{2+} release than 2 μM AdA, as observed. Third, whereas $InsP_3$ invariably stimulated the Ca^{2+}-activated Cl^- current $I_{Cl1\text{-}S}$ (Hartzell, 1996; Hartzell et al., 1997; Kuruma and Hartzell, 1999; Machaca and Hartzell, 1999), AdA was insufficient to stimulate $I_{Cl1\text{-}S}$ but still generate store-operated Ca^{2+} influx (DeLisle et al., 1997; Hartzell et al., 1997; Machaca and Hartzell, 1999). Our experimental results offer a likely explanation. The rate of Ca^{2+} release activated by $InsP_3$ was invariably high enough to activate $I_{Cl1\text{-}S}$ because of the high P_{max} of $InsP_3$-liganded $InsP_3R$ channels. In contrast, in suboptimal cytoplasmic-free ATP concentrations, the reduced P_{max} of the AdA-liganded channels gave rise to a slower rate of Ca^{2+} release that was insufficient to stimulate $I_{Cl1\text{-}S}$. This slow rate of release activated by AdA was nevertheless sufficient over time to deplete the $InsP_3$ sensitive Ca^{2+} stores, thereby generating store-operated Ca^{2+} influx.

Of considerable interest is the possibility to correlate distinct single-channel properties of the $InsP_3R$ activated by either $InsP_3$ or AdA with the distinct kinetics of elementary Ca^{2+} release events (puffs) triggered by these ligands in *Xenopus* oocytes. Puffs mediated by the *X*-$InsP_3R$-1 have been imaged in oocytes activated sequentially by $InsP_3$ and AdA (Marchant and Parker, 1998). These spatially restricted puffs reflect the activation of several $InsP_3R$ channels within a cluster of channels. The variable amplitudes of puffs can be understood as reflecting variable numbers of $InsP_3R$ channels within clusters (Mak and Foskett, 1997; Sun et al., 1998; Thomas et al., 1998) and the stochastic nature of the channel gating (Mak and Foskett, 1997). Puffs have been characterized by quantitative determinations of the peak change in fluorescence, as a measure of the peak rate of Ca^{2+} liberation; the duration and the rise time, both reflecting the length of time the channels were open to release Ca^{2+}; and signal mass, representing the total amount of Ca^{2+} released (Marchant and Parker, 1998; Sun et al., 1998). A major unresolved question in calcium signaling is the nature of the mechanisms that regulate the duration of Ca^{2+} release during a puff. Puffs elicited by activation with low concentrations of AdA had similar peak rates of Ca^{2+} liberation but were temporally shorter (faster rise time and shorter duration) and released less total Ca^{2+} compared with those activated by $InsP_3$ (Marchant and Parker, 1998). The principle conclusion from these results was that the duration of a Ca^{2+} puff bears no simple relationship to the affinity of the agonist, ruling out agonist dissociation as the mechanism which delimits the period of Ca^{2+} flux through the $InsP_3R$ channels during a puff (Marchant and Parker, 1998). Therefore, it was speculated (Marchant and Parker, 1998) that Ca^{2+}-mediated inhibition (Parker and Ivorra, 1990; Finch et al., 1991) and $InsP_3$-induced channel inactiva-

tion (Hajnóczky and Thomas, 1994; Mak and Foskett, 1997) may be involved. Our results now suggest another possible mechanism. Our study of the single-channel properties of the *X*-$InsP_3R$-1 has revealed that in suboptimal ATP concentrations, the main difference between $InsP_3R$ channels activated by AdA and $InsP_3$ is the significantly shorter $\langle\tau^o\rangle$ of the AdA-liganded channels (Fig. 10, B and C). Thus, there is a correlation between $\langle\tau^o\rangle$ of the single $InsP_3R$ channel and the rise time, duration, and total amount of Ca^{2+} released of a Ca^{2+} puff. Therefore, we suggest that a major determinant of the duration of Ca^{2+} release, and of the amount of Ca^{2+} released during a puff, is the ligand-dependent $\langle\tau^o\rangle$, rather than Ca^{2+}-mediated inhibition or ligand-induced channel inactivation. It is interesting to note that Ca^{2+} sparks mediated by ryanodine receptor Ca^{2+} release channels in frog skeletal muscle fibers have faster rise times and reduced total Ca^{2+} released when $\langle\tau^o\rangle$ of the channels is prematurely shortened by membrane repolarization (Lacampagne et al., 2000). Thus, $\langle\tau^o\rangle$ can be a major determinant of the duration of elementary Ca^{2+} release events mediated by both major families of intracellular Ca^{2+} release channels.

Based on our studies of the regulation of the single-channel activities of *X*-$InsP_3R$-1, we consider the following scenario as one that can account for the correlation between $\langle\tau^o\rangle$ and the duration of a puff. It is generally believed that each Ca^{2+} puff is initiated by the stochastic opening of one of the $InsP_3R$ channels clustered together in the Ca^{2+} release site (Yao et al., 1995). The Ca^{2+} released by one channel can diffuse to neighboring channels, increasing the local $[Ca^{2+}]_i$ in the vicinity of those channels so that they too open, by Ca^{2+} activation (Ca^{2+} induced Ca^{2+} release). Other mechanisms may serve to couple the channels to affect a concerted opening of several of them (Mak and Foskett, 1997; Marx et al., 1998). This rapid concerted activation of the channels in a cluster generates the Ca^{2+} puffs (Yao et al., 1995; Mak and Foskett, 1997; Sun et al., 1998). The locally high $[Ca^{2+}]_i$ near the channels as a result of this liberation can, in turn, feed back to inhibit them (Figs. 3, 4, and 7). Indeed, because puffs are generated under conditions of low agonist concentration (Yao et al., 1995; Berridge, 1997; Marchant and Parker, 1998), the channel has a high sensitivity to Ca^{2+} inhibition (Mak et al., 1998; and this study). Nevertheless, a critical observation is that $\langle\tau^o\rangle$ has very little dependence on $[Ca^{2+}]_i$ (Fig. 10). This lack of sensitivity of the open channel to Ca^{2+} inhibition implies that, once a channel has opened, it will stay open for a duration approximately equal to $\langle\tau^o\rangle$, independent of the local $[Ca^{2+}]_i$ in the vicinity of the channel. Only after the channel closes can cytoplasmic Ca^{2+} feed back to inhibit it from reopening, as Ca^{2+} inhibition of gating operates by stabilizing the channel closed state (Fig. 10). Thus, once a channel has opened during a puff, it will stay open for a duration approximately equal to $\langle\tau^o\rangle$ and then close. At that time, it is possible that the high local $[Ca^{2+}]_i$, contributed by Ca^{2+} released from the channel itself as well as from its neighbors, will prevent it from reopening within the duration of the puff. Therefore, during a single puff, each channel in the Ca^{2+} release site likely opens at most once. As the conductance properties of the AdA- and $InsP_3$-liganded channels are indistinguishable (Fig. 2), the mean amount of Ca^{2+} released in an opening of each $InsP_3R$ channel in a cluster is therefore predicted to be directly proportional to $\langle\tau^o\rangle$. This model also predicts that the mean duration of the puff will be proportional to $\langle\tau^o\rangle$.

Alternatively, the puff could terminate as a result of the stochastic nature of channel gating without invoking Ca^{2+} inhibition of reopening. When all the activated channels in the cluster become closed at the same time, simply as a result of the nonzero probability that the stochastic closed times of all the activated channels will coincide, the Ca^{2+} release needed for stimulation of further openings will be eliminated, thereby extinguishing the puff (Niggli, 1999; Stern et al., 1999). This model is similar to the stochastic attrition model developed by Stern (1992) to help account for termination of Ca^{2+} release through clusters of ryanodine receptors. Analytical derivation of the time constant for the puff duration in the stochastic attrition model showed it to be directly proportional to the channel mean open duration (Stern et al., 1999). Thus, models using Ca^{2+} inhibition or stochastic attrition both suggest that the difference between the duration of puffs and the quantities of Ca^{2+} released by puffs activated by $InsP_3$ and AdA (Marchant and Parker, 1998) is a consequence of the difference in the mostly Ca^{2+}-independent $\langle\tau^o\rangle$ of the $InsP_3$- and AdA-liganded $InsP_3R$ channels. Importantly, our results demonstrate that this difference is a function of the cytoplasmic free ATP concentration, suggesting that free ATP concentration helps to shape the properties of elementary Ca^{2+} release signals generated by AdA.

This work was supported by grants to J.K. Foskett from the National Institutes of Health (MH59937 and GM56328) and to D.-O.D. Mak from the American Heart Association (9906220U).

Submitted: 21 December 2000
Revised: 12 February 2001
Accepted: 13 February 2001

REFERENCES

Adkins, C.E., S.A. Morris, H. De Smedt, I. Sienaert, K. Török, and C.W. Taylor. 2000. Ca^{2+}-calmodulin inhibits Ca^{2+} release mediated by type-1,-2 and-3 inositol trisphosphate receptors. *Biochem. J.* 345:357–363.

Baudet, S.B., L. Hove-Madsen, and D.M. Bers. 1994. How to make and use calcium-specific mini- and microelectrodes. *In* A Practical Guide to the Study of Calcium in Living Cells. R. Nuccitelli,

editor. Academic Press, San Diego, CA. 94–114.

Beecroft, M.D., J.S. Marchant, A.M. Riley, N.C.R. Van Straten, G.A. Van der Marel, J.H. Van Boom, B.V.L. Potter, and C.W. Taylor. 1999. Acyclophostin: a ribose-modified analog of adenophostin A with high affinity for inositol 1,4,5-trisphosphate receptors and pH-dependent efficacy. *Mol. Pharmacol.* 55:109–117.

Berridge, M.J. 1997. Elementary and global aspects of calcium signalling. *J. Physiol.* 499:291–306.

Bezprozvanny, I., J. Watras, and B.E. Ehrlich. 1991. Bell-shaped calcium-response curves of Ins(1,4,5)P_3- and calcium-gated channels from endoplasmic reticulum of cerebellum. *Nature.* 351:751–754.

Bezprozvanny, I., and B.E. Ehrlich. 1993. ATP modulates the function of inositol 1,4,5-trisphosphate-gated channels at two sites. *Neuron.* 10:1175–1184.

Bird, G.S., M. Takahashi, K. Tanzawa, and J.W. Putney, Jr. 1999. Adenophostin A induces spatially restricted calcium signaling in *Xenopus laevis* oocytes. *J. Biol. Chem.* 274:20643–20649.

Bootman, M.D., and M.J. Berridge. 1995. The elemental principles of calcium signaling. *Cell.* 83:675–678.

Broad, L.M., D.L. Armstrong, and J.W. Putney, Jr. 1999. Role of the inositol 1,4,5-trisphosphate receptor in Ca^{2+} feedback inhibition of calcium release-activated calcium current (I_{crac}). *J. Biol. Chem.* 274:-32881–32888.

DeLisle, S., E.W. Marksberry, C. Bonnett, D.J. Jenkins, B.V.L. Potter, M. Takahashi, and K. Tanzawa. 1997. Adenophostin A can stimulate Ca^{2+} influx without depleting the inositol 1,4,5-trisphosphate-sensitive Ca^{2+} stores in the *Xenopus* oocyte. *J. Biol. Chem.* 272:9956–9961.

Ferris, C.D., R.L. Huganir, and S.H. Snyder. 1990. Calcium flux mediated by purified inositol 1,4,5-trisphosphate receptor in reconstituted lipid vesicles is allosterically regulated by adenine nucleotides. *Proc. Natl. Acad. Sci. USA.* 87:2147–2151.

Finch, E.A., T.J. Turner, and S.M. Goldin. 1991. Calcium as a coagonist of inositol 1,4,5-trisphosphate-induced calcium release. *Science.* 252:443–446.

Flatman, P.W. 1991. Mechanisms of magnesium transport. *Annu. Rev. Physiol.* 53:259–271.

Glouchankova, L., U.M. Krishna, B.V.L. Potter, J.R. Falck, and I. Bezprozvanny. 2000. Association of the inositol (1,4,5)-trisphosphate receptor ligand binding site with phosphatidylinositol (4,5)-bisphosphate and adenophostin A. *Mol. Cell Biol. Res. Commun.* 3:153–158.

Gregory, R.B., R.A. Wilcox, L.A. Berven, N.C.R. Van Straten, G.A. Van der Marel, J.H. Van Boom, and G.J. Barritt. 1999. Evidence for the involvement of a small subregion of the endoplasmic reticulum in the inositol trisphosphate receptor-induced activation of Ca^{2+} inflow in rat hepatocytes. *Biochem. J.* 341:401–408.

Hagar, R.E., and B.E. Ehrlich. 2000. Regulation of the type III $InsP_3$ receptor by $InsP_3$ and ATP. *Biophys. J.* 79:271–278.

Hajnóczky, G., and A.P. Thomas. 1994. The inositol trisphosphate calcium channel is inactivated by inositol trisphosphate. *Nature.* 370:474–477.

Hartzell, H.C. 1996. Activation of different Cl currents in *Xenopus* oocytes by Ca liberated from stores and by capacitative Ca influx. *J. Gen. Physiol.* 108:157–175.

Hartzell, H.C., K. Machaca, and Y. Hirayama. 1997. Effects of adenophostin-A and inositol-1,4,5-trisphosphate on Cl^- currents in *Xenopus laevis* oocytes. *Mol. Pharmacol.* 51:683–692.

He, C.L., P. Damiani, T. Ducibella, M. Takahashi, K. Tanzawa, J.B. Parys, and R.A. Fissore. 1999. Isoforms of the inositol 1,4,5-trisphosphate receptor are expressed in bovine oocytes and ovaries: the type-1 isoform is down-regulated by fertilization and by injection of adenophostin A. *Biol. Reprod.* 61:935–943.

Hirota, J., T. Michikawa, A. Miyawaki, M. Takahashi, K. Tanzawa, I. Okura, T. Furuichi, and K. Mikoshiba. 1995. Adenophostin-mediated quantal Ca^{2+} release in the purified and reconstituted inositol 1,4,5-trisphosphate receptor type 1. *FEBS Lett.* 368:248–252.

Hotoda, H., K. Murayama, S. Miyamoto, Y. Iwata, M. Takahashi, Y. Kawase, K. Tanzawa, and M. Kaneko. 1999. Molecular recognition of adenophostin, a very potent Ca^{2+} inducer, at the D-*myo*-inositol 1,4,5-trisphosphate receptor. *Biochemistry.* 38:9234–9241.

Huang, Y., M. Takahashi, K. Tanazawa, and J.W. Putney, Jr. 1998. Effect of adenophostin A on Ca^{2+} entry and calcium release-activated calcium current (I_{crac}) in rat basophilic leukemia cells. *J. Biol. Chem.* 273:31815–31821.

Iino, M. 1990. Biphasic Ca^{2+} dependence of inositol 1,4,5-trisphosphate-induced Ca release in smooth muscle cells of the guinea pig taenia caeci. *J. Gen. Physiol.* 95:1103–1122.

Iino, M. 1991. Effects of adenine nucleotides on inositol 1,4,5-trisphosphate-induced calcium release in vascular smooth muscle cells. *J. Gen. Physiol.* 98:681–698.

Irvine, R.F., K.D. Brown, and M.J. Berridge. 1984. Specificity of inositol trisphosphate-induced calcium release from permeabilized Swiss-mouse 3T3 cells. *Biochem. J.* 222:269–272.

Jellerette, T., C.L. He, H. Wu, J.B. Parys, and R.A. Fissore. 2000. Down-regulation of the inositol 1,4,5-trisphosphate receptor in mouse eggs following fertilization or parthenogenetic activation. *Dev. Biol.* 223:238–250.

Kashiwayanagi, M., K. Tatani, S. Shuto, and A. Matsuda. 2000. Inositol 1,4,5-trisphosphate and adenophostin analogues induce responses in turtle olfactory sensory neurons. *Eur. J. Neurosci.* 12:606–612.

Kume, S., A. Muto, J. Aruga, T. Nakagawa, T. Michikawa, T. Furuichi, S. Nakade, H. Okano, and K. Mikoshiba. 1993. The *Xenopus* IP_3 receptor: structure, function, and localization in oocytes and eggs. *Cell.* 73:555–570.

Kuruma, A., and H.C. Hartzell. 1999. Dynamics of calcium regulation of chloride currents in *Xenopus* oocytes. *Am. J. Physiol. Cell Physiol.* 276:C161–C175.

Lacampagne, A., M.G. Klein, C.W. Ward, and M.F. Schneider. 2000. Two mechanisms for termination of individual Ca^{2+} sparks in skeletal muscle. *Proc. Natl. Acad. Sci. USA.* 97:7823–7828.

Landolfi, B., S. Curci, L. Debellis, T. Pozzan, and A.M. Hofer. 1998. Ca^{2+} homeostasis in the agonist-sensitive internal store: functional interactions between mitochondria and the ER measured in situ in intact cells. *J. Cell Biol.* 142:1235–1243.

Machaca, K., and H.C. Hartzell. 1999. Adenophostin A and inositol 1,4,5-trisphosphate differentially activate Cl^- currents in *Xenopus* oocytes because of disparate Ca^{2+} release kinetics. *J. Biol. Chem.* 274:4824–4831.

Maeda, N., T. Kawasaki, S. Nakade, N. Yokota, T. Taguchi, M. Kasai, and K. Mikoshiba. 1991. Structural and functional characterization of inositol 1,4,5-trisphosphate receptor channel from mouse cerebellum. *J. Biol. Chem.* 266:1109–1116.

Maes, K., L. Missiaen, J.B. Parys, I. Sienaert, G. Bultynck, M. Zizi, P. De Smet, R. Casteels, and H. De Smedt. 1999. Adenine-nucleotide binding sites on the inositol 1,4,5-trisphosphate receptor bind caffeine, but not adenophostin A or cyclic ADP-ribose. *Cell Calcium.* 25:143–152.

Mak, D.-O.D., and J.K. Foskett. 1994. Single-channel inositol 1,4,5-trisphosphate receptor currents revealed by patch clamp of isolated *Xenopus* oocyte nuclei. *J. Biol. Chem.* 269:29375–29378.

Mak, D.-O.D., and J.K. Foskett. 1997. Single-channel kinetics, inactivation, and spatial distribution of inositol trisphosphate (IP_3) receptors in *Xenopus* oocyte nucleus. *J. Gen. Physiol.* 109:571–587.

Mak, D.-O.D., S. McBride, and J.K. Foskett. 1998. Inositol 1,4,5-trisphosphate activation of inositol trisphosphate receptor Ca^{2+} channel by ligand tuning of Ca^{2+} inhibition. *Proc. Natl. Acad. Sci. USA.* 95:15821–15825.

Mak, D.-O.D, and J.K. Foskett. 1998. Effects of divalent cations on single-channel conduction properties of *Xenopus* IP_3 receptor.

Am. J. Physiol. 275:C179–C188.

Mak, D.-O.D., S. McBride, and J.K. Foskett. 1999. ATP regulation of type 1 inositol 1,4,5-trisphosphate receptor channel gating by allosteric tuning of Ca^{2+} activation. *J. Biol. Chem.* 274:22231–22237.

Marchant, J.S., M.D. Beecroft, A.M. Riley, D.J. Jenkins, R.D. Marwood, C.W. Taylor, and B.V.L. Potter. 1997. Disaccharide polyphosphates based upon adenophostin A activate hepatic D-*myo*-inositol 1,4,5-trisphosphate receptors. *Biochemistry.* 36:12780–12790.

Marchant, J.S., and I. Parker. 1998. Kinetics of elementary Ca^{2+} puffs evoked in *Xenopus* oocytes by different $Ins(1,4,5)P_3$ receptor agonists. *Biochem. J.* 334:505–509.

Marx, S.O., K. Ondrias, and A.R. Marks. 1998. Coupled gating between individual skeletal muscle Ca^{2+} release channels (ryanodine receptors). *Science.* 281:818–821.

Meas, K., L. Missiaen, P. De Smet, G. Vanlingen, G. Callewaert, J.B. Parys, and H. De Smedt. 2000. Differential modulation of inositol 1,4,5-trisphosphate receptor type 1 and type 3 by ATP. *Cell Calcium.* 27:257–267.

Meyer, T., D. Holowka, and L. Stryer. 1988. Highly cooperative opening of calcium channels by inositol 1,4,5-trisphosphate. *Science.* 240:653–655.

Mignery, G.A., T.C. Sudhof, K. Takei, and P. De Camilli. 1989. Putative receptor for inositol 1,4,5-trisphosphate similar to ryanodine receptor. *Nature.* 342:192–195.

Mikoshiba, K. 1993. Inositol 1,4,5-trisphosphate receptor. *Trends Pharmacol. Sci.* 14:86–89.

Missiaen, L., J.B. Parys, H. De Smedt, I. Sienaert, H. Sipma, S. Vanlingen, K. Maes, and R. Casteels. 1997. Effect of adenine nucleotides on *myo*-inositol-1,4,5-trisphosphate-induced calcium release. *Biochem. J.* 325:661–666.

Missiaen, L., J.B. Parys, I. Sienaert, K. Maes, K. Kunzelmann, M. Takahashi, K. Tanzawa, and H. De Smedt. 1998. Functional properties of the type-3 $InsP_3$ receptor in 16HBE14o- bronchial mucosal cells. *J. Biol. Chem.* 273:8983–8986.

Murphy, C.T., A.M. Riley, C.J. Lindley, D.J. Jenkins, J. Westwick, and B.V.L. Potter. 1997. Structural analogues of D-*myo*-inositol-1,4,5-trisphosphate and adenophostin A: recognition by cerebellar and platelet inositol-1,4,5-trisphosphate receptors. *Mol. Pharmacol.* 52:741–748.

Niggli, E. 1999. Localized intracellular calcium signaling in muscle: calcium sparks and calcium quarks. *Annu. Rev. Physiol.* 61:311–335.

Parker, I., and I. Ivorra. 1990. Inhibition by Ca^{2+} of inositol trisphosphate-mediated Ca^{2+} liberation: a possible mechanism for oscillatory release of Ca^{2+}. *Proc. Natl. Acad. Sci. USA.* 87:260–264.

Shuto, S., K. Tatani, Y. Ueno, and A. Matsuda. 1998. Synthesis of adenophostin analogues lacking the adenine moiety as novel potent IP_3 receptor ligands: some structural requirements for the significant activity of adenophostin A. *J. Org. Chem.* 63:8815–8824.

Sigworth, F.J., and S.M. Sine. 1987. Data transformations for improved display and fitting of single channel dwell time histograms. *Biophys. J.* 52:1047–1054.

Stern, M.D. 1992. Theory of excitation-contraction coupling in cardiac muscle. *Biophys. J.* 63:497–517.

Stern, M.D., L.S. Song, H.P. Cheng, J.S.K. Sham, H.T. Yang, K.R. Boheler, and E. Ríos. 1999. Local control models of cardiac excitation-contraction coupling. A possible role for allosteric interactions between ryanodine receptors. *J. Gen. Physiol.* 113:469–489.

Sun, X.-P., N. Callamaras, J.S. Marchant, and I. Parker. 1998. A continuum of $InsP_3$-mediated elementary Ca^{2+} signalling events in *Xenopus* oocytes. *J. Physiol.* 509:67–80.

Takahashi, M., K. Tanzawa, and S. Takahashi. 1994. Adenophostins, newly discovered metabolites of *Penicillium brevicompactum*, act as potent agonists of the inositol 1,4,5-trisphosphate receptor. *J. Biol. Chem.* 269:369–372.

Thomas, D., P. Lipp, M.J. Berridge, and M.D. Bootman. 1998. Hormone-evoked elementary Ca^{2+} signals are not stereotypic, but reflect activation of different size channel clusters and variable recruitment of channels within a cluster. *J. Biol. Chem.* 273:27130–27136.

Toescu, E.C. 1995. Temporal and spatial heterogeneities of Ca^{2+} signaling: mechanisms and physiological roles. *Am. J. Physiol.* 269: G173–G185.

Vanlingen, S., H. Sipma, P. De Smet, G. Callewaert, L. Missiaen, H. De Smedt, and J.B. Parys. 2000. Ca^{2+} and calmodulin differentially modulate *myo*-inositol 1,4,5-trisphosphate (IP_3)-binding to the recombinant ligand-binding domains of the various IP_3 receptor isoforms. *Biochem. J.* 346:275–280.

Wilcox, R.A., C. Erneux, W.U. Primrose, R. Gigg, and S.R. Nahorski. 1995. 2-hydroxyethyl a-D-glucopyranoside 2,3',4'-trisphosphate: a novel metabolically resistant adenophostin A and *myo*-inositol 1,4,5-trisphosphate analogue potently interacts with the *myo*-inositol 1,4,5-trisphosphate receptor. *Biochem. Soc. Trans.* 23:420S.

Yao, Y., J. Choi, and I. Parker. 1995. Quantal puffs of intracellular Ca^{2+} evoked by inositol trisphosphate in *Xenopus* oocytes. *J. Physiol.* 482:533–553.